CORE
Metadata, citation and similar papers at core.ac.uk
Provided by University of Regensburg Publication Server

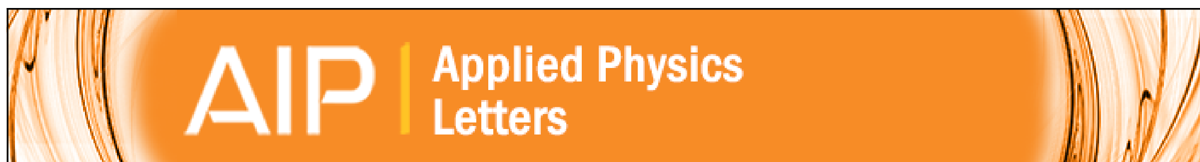

In-plane tunneling anisotropic magnetoresistance in (Ga,Mn)As/GaAs Esaki diodes in the regime of the excess current

J. Shiogai, M. Ciorga, M. Utz, D. Schuh, M. Kohda, D. Bougeard, T. Nojima, D. Weiss, and J. Nitta

Citation: Applied Physics Letters **106**, 262402 (2015); doi: 10.1063/1.4923309
View online: http://dx.doi.org/10.1063/1.4923309
View Table of Contents: http://scitation.aip.org/content/aip/journal/apl/106/26?ver=pdfcov
Published by the AIP Publishing

Articles you may be interested in
Impact of current paths on measurement of tunneling magnetoresistance and spin torque critical current densities in GaMnAs-based magnetic tunnel junctions
J. Appl. Phys. **113**, 083702 (2013); 10.1063/1.4793086

Anisotropic magneto-resistance in a GaMnAs-based single impurity tunnel diode: A tight binding approach
Appl. Phys. Lett. **100**, 062403 (2012); 10.1063/1.3683525

Local spin valve effect in lateral (Ga,Mn)As/GaAs spin Esaki diode devices
AIP Advances **1**, 022113 (2011); 10.1063/1.3591397

Tunneling anisotropic spin polarization in lateral (Ga,Mn)As/GaAs spin Esaki diode devices
Appl. Phys. Lett. **95**, 152101 (2009); 10.1063/1.3247187

Tunneling anisotropic magnetoresistance: Creating a spin-valve-like signal using a single ferromagnetic semiconductor layer
J. Appl. Phys. **97**, 10C506 (2005); 10.1063/1.1848353

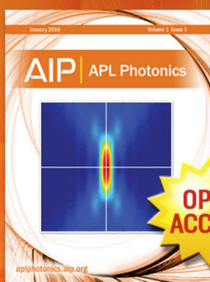

Launching in 2016!
The future of applied photonics research is here
AIP APL Photonics

This article is copyrighted as indicated in the article. Reuse of AIP content is subject to the terms at: http://scitation.aip.org/termsconditions. Downloaded to IP: 132.199.100.37 On: Thu, 02 Jul 2015 10:36:54

In-plane tunneling anisotropic magnetoresistance in (Ga,Mn)As/GaAs Esaki diodes in the regime of the excess current

J. Shiogai,[1,2] M. Ciorga,[3,a)] M. Utz,[3] D. Schuh,[3] M. Kohda,[1] D. Bougeard,[3] T. Nojima,[2] D. Weiss,[3] and J. Nitta[1]
[1]*Department of Materials Science, Tohoku University, Sendai 980-8579, Miyagi, Japan*
[2]*Institute of Materials Research, Tohoku University, Sendai 980-8577, Miyagi, Japan*
[3]*Institute of Experimental and Applied Physics, University of Regensburg, D-93040 Regensburg, Germany*

(Received 27 February 2015; accepted 19 June 2015; published online 29 June 2015)

We investigate the angular dependence of the tunneling anisotropic magnetoresistance in (Ga,Mn)As/*n*-GaAs spin Esaki diodes in the regime where the tunneling process is dominated by the excess current through midgap states in (Ga,Mn)As. We compare it to similar measurements performed in the regime of band-to-band tunneling. Whereas the latter show biaxial symmetry typical for magnetic anisotropy observed in (Ga,Mn)As samples, the former is dominated by uniaxial anisotropy along the ⟨110⟩ axes. © *2015 AIP Publishing LLC*.
[http://dx.doi.org/10.1063/1.4923309]

A ferromagnetic/nonmagnetic (FM/NM) junction constitutes a fundamental building block of many spintronic devices.[1] One of its common applications is to generate and detect spin accumulations in NM materials by electrical means.[2,3] In order to achieve high values of spin injection efficiency such a junction should be operated in the tunneling regime, especially when the NM is a semiconductor.[4,5] This is often realized by inserting a thin insulating layer between FM and NM. In recent years there has been a great interest in investigating the role of impurities in such junctions,[6–8] localized within the tunnel barrier or on either side of it, on the spin transport through such a device. Much of the interest has been caused by the recent controversies regarding the so-called three-terminal (3 T) method of spin detection,[6–9] where one and the same contact is used to inject and detect spins in a NM. This method has been particularly employed to investigate spin injection in group IV materials,[10] but its validity has been widely disputed.[11–14] High signals, which have been recorded using the 3 T method, are often assigned to spin accumulation generated in localized states at the junction, or simply to magnetoresistance effects originating from the inelastic tunneling through impurities present in such a junction. Recently, we have investigated the influence of localized states in the gap of the ferromagnetic semiconductor (Ga,Mn)As on the spin signal observed in (Ga,Mn)As/GaAs spin Esaki diode devices.[15] Although we have shown that the measured 3 T signal contains qualitative information about the spin accumulation generated in the channel, its amplitude depends on the bias-dependent spin detection sensitivity.[16] This puts into question the validity of the 3 T method as a straightforward tool for spin injection studies. The discrepancy between the amplitude of the 3 T signal and the actual spin accumulation is particularly strong in the region when the tunneling is dominated by the excess current through localized states in the gap of (Ga,Mn)As.

a)Author to whom correspondence should be addressed. Electronic mail: mariusz.ciorga@ur.de

In this letter, we further investigate the role of localized gap states in tunneling through the (Ga,Mn)As/GaAs Esaki diode. We study the tunneling anisotropic magnetoresistance effect (TAMR) of our structure in and outside the regime of excess current flow. TAMR is one of the novel magnetoresistance effects discovered in a (Ga,Mn)As-based tunnel junction[17] and later observed in junctions with metal ferromagnets.[18] The core of the effect is the dependence of the resistance of the junction on the magnetization orientation of the ferromagnetic layer. In (Ga,Mn)As, the effect is ascribed to the combined contribution of spin-orbit and exchange interactions, resulting in density of states anisotropies[17] and thus magnetization dependent shifts of the Fermi level.[19,20] In the past, we have investigated TAMR in Esaki diode structures in the regime of band-to-band tunneling.[21,22] We observed the typical symmetry of magnetic anisotropies in (Ga,Mn)As-based transport devices: a dominating cubic anisotropy along the ⟨100⟩ crystal directions, accompanied by a superimposed uniaxial anisotropy along the ⟨110⟩ directions.[23] The cubic anisotropy reflects the T_d symmetry of the zinc-blend crystal, whereas the uniaxial anisotropy is the signature of reducing this symmetry to C_{2v}. In bulk (Ga,Mn)As a non-uniform distribution of Mn dimers along the ⟨110⟩ directions of the epitaxially grown surface is named as a possible origin of this symmetry reduction,[24] whereas in case of heterostructures it reflects an asymmetry of the corresponding interfaces. In contrast, the symmetry of the TAMR effect observed here in the excess current regime is completely dominated by the uniaxial anisotropy, with maximum resistance observed for the [1$\bar{1}$0] direction and minimum for the [110] direction. To make sure that this uniaxial anisotropy is not dominated by the tunneling anisotropic spin polarization (TASP), which exhibits a similar uniaxial symmetry,[22,25] we also measured TASP using a nonlocal spin-detection technique.

Data presented in this work were obtained from a sample fabricated from the same epitaxial wafer that was used before for other spin-related investigations.[26] The wafer was grown on a semi-insulating GaAs (001) substrate, consisting

 © 2015 AIP Publishing LLC

This article is copyrighted as indicated in the article. Reuse of AIP content is subject to the terms at: http://scitation.aip.org/termsconditions. Downloaded to IP: 132.199.100.37 On: Thu, 02 Jul 2015 10:36:54

of a 300 nm GaAs buffer layer, a 500 nm thick (Al,Ga)As/GaAs superlattice, 1 μm n-GaAs, 15 nm $n \rightarrow n^+$-GaAs transition layer, 8.0 nm n^+-GaAs, 2.2 nm (Al,Ga)As diffusion barrier, and 50 nm (Ga,Mn)As. The corresponding doping concentrations are $n = 2 \times 10^{16}\,\mathrm{cm}^{-3}$ and $n^+ = 5 \times 10^{18}\,\mathrm{cm}^{-3}$. The wafer was patterned into a 50–μm-wide mesa oriented along the [110] crystallographic direction by standard photolithography and wet chemical etching techniques. Electron beam lithography, Ti/Au evaporation, and reactive ion etching were employed to define ferromagnetic electrodes along the $[1\bar{1}0]$ direction, each of which could be used as a spin injecting or detecting contact. Consistent results to the ones presented here were also obtained from measurements on a different samples, used for 3 T investigations described elsewhere,[15] which was fabricated from a slightly different wafers.

A schematic of the final sample geometry is displayed in Fig. 1(a). Although the investigated samples have five FM contacts on top of the channel, for simplicity, only two are shown in the figure. For MR measurements, a current I_{inj} is driven between a given FM contact and the ground contact at the left edge of the channel, while the three-terminal (3 T) voltage (denoted as V_{3T}) is measured between this contact and the reference electrode at the right edge of the channel. This voltage is a measure of the voltage drop across the junction and, for a constant current, is a direct measure of the resistance of the junction. The spin accumulation, generated in the channel as a result of spin injection, has been probed non-locally by measuring the voltage V_{NL} between the nearby second FM contact and the reference one at the right edge of the channel. All transport measurements in this experiment were performed at $T = 4.2$ K.

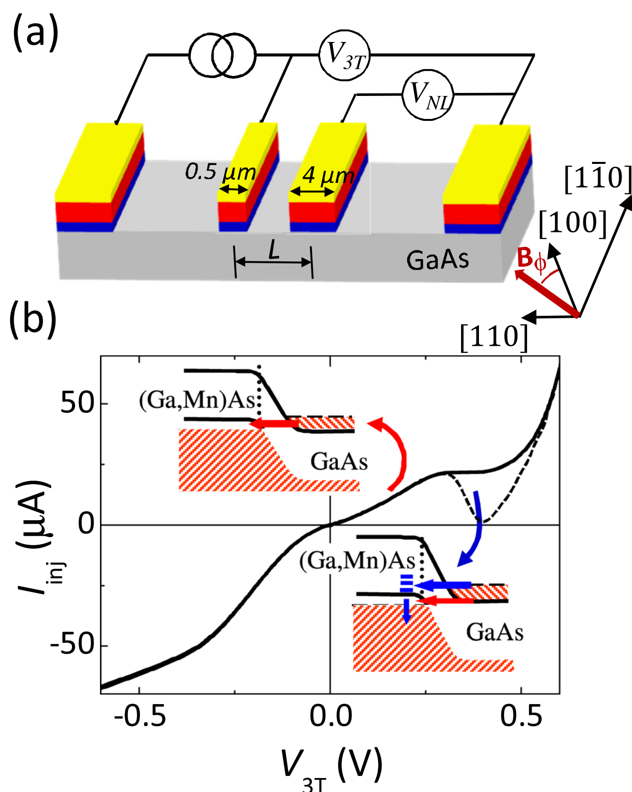

FIG. 1. (a) Schematic device layout and measurement configuration (not to scale). For simplicity only two FM contacts are shown. (b) *I-U* characteristic of the 0.5 μm wide contact measured in the three-terminal configuration. Upper inset: direct band-to-band tunneling (red arrow) dominating at negative and low positive bias values. Lower inset: the excess current (blue arrow) through gap states dominates transport through the Esaki diode close to the Esaki feature. The dashed curve shows a typical *I-U* curve of the Esaki diode in the absence of the excess current.

The current-voltage characteristic of the 0.5 μm wide Esaki diode contact, measured in 3 T configuration, is shown in Fig. 1(b). The current through an Esaki diode consists typically of different contributions from: (i) direct tunneling between the valence band of p–(Ga,Mn)As and the conduction band of n-GaAs; (ii) tunneling through localized states in the bandgap (constituting the so-called excess current[27]); and (iii) thermal transport across the built-in potential. The last component, not interesting for spin injection, dominates at high forward bias. At reverse bias and for small forward bias, on the other hand, the component (i) dominates the current as electrons tunnel from (Ga,Mn)As into GaAs (reverse bias) or in the opposite direction (forward bias). The latter case is schematically shown in the upper inset of Fig. 1(b). This component is suppressed by a further increase of the forward bias, which removes the overlap of the bands. For an ideal Esaki diode, this would lead to a vanishing current and result in the well-known peak-valley structure or a dip in the *I–U* characteristic (see the dashed curve in Fig. 1(b)). In real devices, however, the component (ii) dominates in this regime and is responsible for a non-zero tunnel current. The importance of this process in our devices is manifested by a very shallow Esaki dip observed typically in measured *I–U* characteristics. In case of the one shown in Fig. 1(b), it is not even a dip but rather a flat region between 0.3 and 0.4 V in Fig. 1(b). The process responsible for this behavior is depicted in the lower inset of Fig. 1(b), showing electrons tunneling from the conduction band either into localized states or directly into the valence band. In the following paragraphs we discuss different anisotropy patterns observed in magnetoresistance measured in those two tunneling regimes.

The in-plane TAMR measurements were performed by rotating the external magnetic field $B = 1$ T, sufficiently strong to align the magnetization of the (Ga,Mn)As ferromagnetic electrode along the field, while measuring V_{3T}. The measurements were conducted for different bias currents corresponding to different regimes of tunneling through the Esaki diode. The results are summarized in Fig. 2. Typical TAMR curves obtained in the regime (i), dominated by tunneling between the valence band of (Ga,Mn)As and the conduction band of GaAs, i.e., for $I_{inj} < +10\,\mu$A ($V_{3T} < +0.148$ V) are shown in Fig. 2(a). The TAMR is defined here with respect to the minimum resistance by $TAMR(\phi) = 100\% \times (R_{3T}(\phi) - R_{3T}^{min.})/R_{3T}^{min.}$, where $R_{3T} = V_{3T}/I_{inj}$. The direction of the magnetic field ϕ is defined by the angle between the applied magnetic field and the [100] crystallographic direction of the GaAs substrate. Similarly, as in previous works,[21,22,25] a cubic (biaxial) anisotropy in R_{3T} between $\langle 100\rangle$ and $\langle 110\rangle$ crystallographic directions dominates the picture. A small contribution from a uniaxial anisotropy, breaking the equivalence between [110] and $[1\bar{1}0]$ directions, is also present. The strength and the sign of this uniaxial component strongly depend on bias. For $I_{inj} = -20\,\mu$A ($V_{3T} = -0.166$ V) resistance measured in [110]

This article is copyrighted as indicated in the article. Reuse of AIP content is subject to the terms at: http://scitation.aip.org/termsconditions. Downloaded to IP: 132.199.100.37 On: Thu, 02 Jul 2015 10:36:54

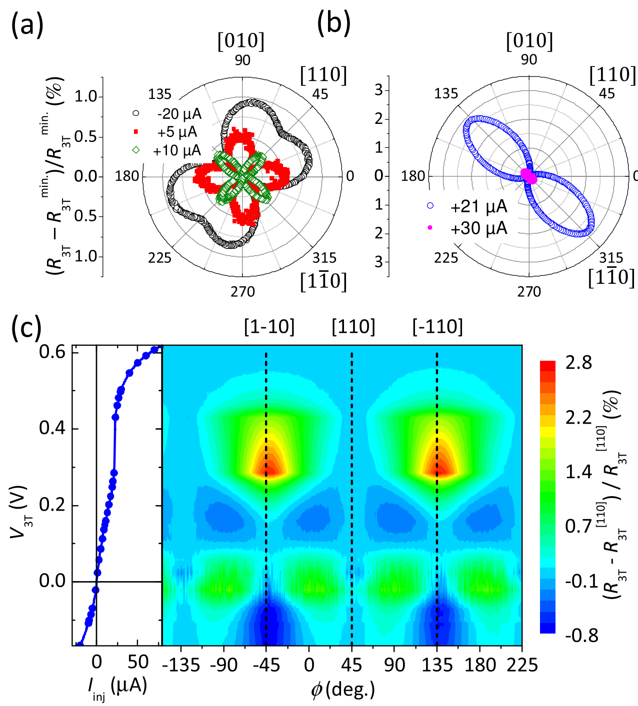

FIG. 2. Dependence of the R_{3T} resistance on the angle ϕ between the external magnetic field B = 1 T and the [100] crystallographic direction. (a) Tunneling anisotropic magnetoresistance (TAMR) normalized to the minimum resistance R_{3T}^{min} for injection currents of $I_{inj} = -20$, +5, and +10 μA ($V_{3T} = -0.166$, +0.086, and 0.148 V, respectively), i.e., in the regime of direct band-to-band tunneling. (b) As in (a) but for injection currents $I_{inj} = +21$ and +30 μA ($V_{3T} = +0.284$ and +0.504 V), i.e., in the presence of the excess current through impurity states. (c) Color-coded plot of the TAMR normalized to the resistance $R_{3T}^{[110]}$ for $B \parallel [110]$ vs angle ϕ and the three-terminal voltage V_{3T}. The plot has been assembled from the angle scans for bias voltage (current) marked with solid circles at *I-U* curve, as shown in the left panel. The color levels between the actual data points have been extrapolated.

direction is ~0.75% larger than in a case of [1$\bar{1}$0] direction, with the latter being also a direction of a total minimum in R_{3T}. For positive bias this uniaxial anisotropy is significantly smaller with a difference in R_{3T} between [1$\bar{1}$0] and [110] directions being ~0.1% for both +5 μA (0.086 V) and +10 μA (0.148 V). The sign of the anisotropy has, however, changed as higher resistance is now measured along the [1$\bar{1}$0] direction. A similar change of sign of the uniaxial TAMR with applied bias has been observed for Fe/GaAs heterostructures, and has been there explained by the combined effect of Bychkov-Rashba and Dresselhaus spin-orbit interaction[18,28] at an interface with reduced C_{2v} symmetry. It is interesting to note that for $I_{inj} = +10$ μA, the cubic anisotropy has an opposite sign compared to the one described previously for the case of negative bias, as R_{3T} becomes higher for the magnetization aligned along ⟨110⟩ directions than for the case of ⟨100⟩ alignment.

Symmetry of the TAMR becomes significantly different when the excess current dominates over direct interband tunneling, i.e., close to the Esaki dip. The uniaxial anisotropy now completely dominates the picture, as it is shown in Fig. 2(b), where curves for $I_{inj} = 21$ μA and 30 μA are displayed. This change of symmetry from a cubic-dominated picture to a uniaxial-dominated one in the region of the excess current is clearly seen in Fig. 2(c), where we plot the TAMR obtained for different bias voltages vs V_{3T} and ϕ as a color-coded plot. Here, magnetoresistance is normalized with respect to $R_{3T}^{[110]}$, corresponding to R_{3T} measured when the magnetic field of 1 T is applied along the [110] direction. For $V_{3T} \lesssim +0.16$ V, ($I_{inj} \lesssim +11$ μA), i.e., in the band-to-band tunneling regime, the fourfold symmetry fully dominates the picture. Approximately at this voltage the onset of a strong uniaxial anisotropy along ⟨110⟩ is observed, which is becoming stronger with increasing voltage, reaching a maximum of 2.8% at $V_{3T} = +0.284$ V ($I_{inj} = +21$ μA). This anisotropy becomes then smaller at higher voltages, when the thermal transport across the built-in potential becomes dominant; the fourfold anisotropy is not present anymore in this regime. One can thus clearly associate the observed change of symmetry in the magnetoresistance with the change of the tunneling mechanism from the band-to-band mechanism to the one dominated by tunneling through impurity states within the gap. It is not likely that the uniaxial anisotropy caused by a non-uniform Mn dimer distribution would be enhanced in the regime of the excess current; therefore, the involvement of the impurity in the tunneling is probably responsible for the uniaxial symmetry. Such a conclusion is consistent with a theoretical report on tunneling in a system involving a single Mn impurity in GaAs:Mn/Al(Ga,As)/*p*-GaAs junction.[29] There it was shown that the tunneling current from the fundamental hole state attached to a single Mn dopant in a GaAs host matrix, coupled to a reservoir through an AlGaAs tunnel barrier shows C_{2v} symmetry with pronounced differences between [1$\bar{1}$0] and [110] directions. The substantial contribution of impurity states detached from the valence band to the tunneling current in the excess regime was shown in other theoretical calculations.[30]

It is well established that resistance measured across an FM/NM junction has a contribution originating from the spin accumulation μ generated in the NM material; the fact utilized in the 3 T method of spin detection. The measured resistance can be generally written as $R_{3T} = R_{3T}^0 + \delta R_{3T}^\mu$, where the first and the second component correspond to the tunnel resistance and to the spin-accumulation-related resistance, respectively. R_{3T}^0 depends on the magnetization direction of the FM layer, due to TAMR effect.[17,18] According to the standard model of spin injection $\delta R_{3T}^\mu = P^2 \rho \lambda / 2S$, where λ is the spin diffusion length in the channel and ρ and S are its resistivity and cross section area, respectively.[5] P is the spin injection efficiency of a given contact, which for tunneling contacts is equal to the tunneling spin polarization (TSP), constituting a spin selectivity of the junction. TSP also depends on magnetization and similarly as TAMR one can define tunneling anisotropic spin polarization as $TASP(\phi) = \Delta P(\phi)/P$. In general, TSP and R_{3T}^0 can be treated as independent parameters of the junction, and therefore, TASP and TAMR can have a different symmetry. In fact, in our earlier work,[22,25] we have shown that the TSP shows a uniaxial anisotropy in (Ga,Mn)As/GaAs Esaki diodes, which were also confirmed by theoretical calculations.[31] Using all above equations and assuming isotropic λ, one can write $\Delta R_{3T} = \Delta R_{3T}^0 + \Delta R_{3T}^\mu$, $\Delta R_{3T}^\mu = 2(\Delta P/P)\delta R_{3T}^\mu = 2TASP \cdot \delta R_{3T}^\mu$. Finally, the measured TAMR can be written as

This article is copyrighted as indicated in the article. Reuse of AIP content is subject to the terms at: http://scitation.aip.org/termsconditions. Downloaded to IP: 132.199.100.37 On: Thu, 02 Jul 2015 10:36:54

$$\text{TAMR} = \Delta R_{3T}/R_{3T} = \Delta R^0_{3T}/R_{3T} + 2TASP \times \delta R^{\mu}_{3T}/R_{3T}. \quad (1)$$

The TASP contributes thus to TAMR with a weight given by $2 \cdot \delta R^{\mu}_{3T}/R_{3T}$. In Ref. 15, we have shown that in (Ga,Mn)As/GaAs spin Esaki diodes, the spin-related component δR^{μ}_{3T} is strongly enhanced in the region of the excess current, mainly because of the enhanced sensitivity of the 3 T detection due to a strong nonlinearity of the *I–U* curve. In order to check whether the uniaxial anisotropy observed in R_{3T} is not caused by TASP but is indeed directly related to TAMR effect in R^0_{3T}, one should then evaluate TASP and its contribution to the total TAMR given by $\delta R^{\mu}_{3T}/R_{3T}$.

To measure the TASP-induced anisotropy in the spin signal, we used the nearby Esaki diode contact to monitor the spin accumulation in the channel using the nonlocal configuration, as shown in Fig. 1(a). The nonlocal voltage V_{NL} was measured together with V_{3T} during the TAMR measurements described above. According to the standard model of spin injection,[4,5] the nonlocal voltage is given by $V_{NL} = (I_{inj}P_1P_2\rho\lambda/2S)\exp(-L/\lambda)$, where L is the distance between injector and detector and $P_{1(2)}$ is the spin injection efficiency of the injector (detector) contacts. Assuming that λ is isotropic, the observed anisotropy in V_{NL} is proportional to the TASP of both involved contacts so that $\Delta V_{NL}/V_{NL} = \Delta P_1/P_1 + \Delta P_2/P_2 = TASP_1 + TASP_2$. In Figs. 3(a) and 3(b), we plot the dependence of the nonlocal resistance $R_{NL} = V_{NL}/I_{inj}$ on the angle ϕ, obtained simultaneously with the TAMR curves, as shown in Fig. 2. The data display a strong uniaxial anisotropy with the maximum signal along the $[1\bar{1}0]$ direction. This is consistent with our previous experiments[22,25] as well as with theoretical calculations.[31] Both the sign and the strength of the anisotropy, being around 20%, are barely influenced by the applied bias in the explored range. Therefore, we can assume that $TASP_1 = TASP_2 = TASP$, what allows us to evaluate the TASP of one contact as ~10%, the value consistent with our previous reports.

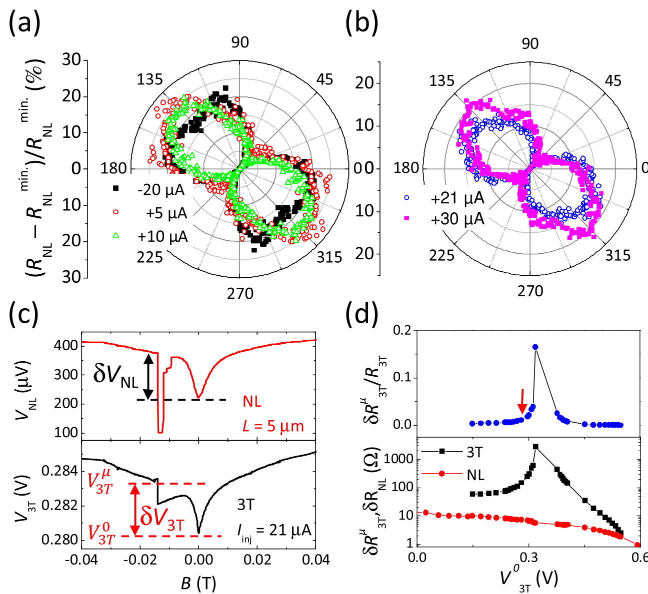

FIG. 3. (a) Anisotropy of the nonlocal resistance $R_{NL}(\phi)$, measured at the detector placed $L = 20\,\mu$m from the injector, normalized to the minimum value, plotted as a function of the angle ϕ for $B = 1$ T. Injection currents are the same as in Fig. 2(a) for 3 T measurements. (b) As in (a) but with injection currents as in Fig. 2(b). (c) Nonlocal voltage V_{NL} (top panel) and three-terminal voltage V_{3T} (bottom panel) as a function of the in-plane magnetic field $B \parallel [1\bar{1}0]$, swept from positive to negative values. The spin injection current was $I_{inj} = +21\,\mu$A ($V_{3T} = +0.280$ V). Spin signals δV_{NL} and δV_{3T} were extracted from the DNP feature around $B = 0$. (d) Bottom: bias dependence of the detected spin signal $\delta R_{3T(NL)} = \delta V_{3T(NL)}/I_{inj}$ in 3 T (black squares) and NL (red circles) geometries. V_{NL} is measured at $L = 5\,\mu$m. Top: the contribution of the spin-accumulation-induced resistance δR^{μ}_{3T} to the total resistance of the junction R_{3T}. The arrow points to the value corresponding to $I_{inj} = +21\,\mu$A, for which maximum TAMR = 2.8% was observed.

To check if the ~10% TASP might be responsible for the anisotropy in R_{3T}, as displayed in Fig. 2, we independently measured the amplitude of the spin-accumulation-related signal δR^{μ}_{3T} and its contribution to R_{3T} performing experiments in the spin-valve configuration,[32] i.e., with a magnetic field swept along the contacts. Figure 3(c) shows NL voltage for detector at $L = 5\,\mu$m and 3 T voltage as a function of such a field for $I_{inj} = 21\,\mu$A. The NL voltage shows clearly a spin-valve signal corroborating spin accumulation in the GaAs channel. As a measure of spin accumulation we use the amplitude of a feature around B = 0, arising from depolarization of the spins due to dynamic nuclear polarization (DNP) effects in GaAs.[33] We denote this amplitude as δV_{NL} and δV_{3T} in Fig. 3(c), for nonlocal and 3 T configuration, respectively. The validity of the method is confirmed when one compares δV_{NL} and δV_{3T} with corresponding Hanle measurements,[15,32] or with a SV signal [see Fig. 3(c)]. This method is particularly useful in case of 3 T measurements, where in-plane B-field sweeps can be used to detect the spin accumulation instead of the time consuming Hanle measurements. The corresponding amplitudes $\delta R^{\mu}_{3T} = \delta V_{3T}/I_{inj}$ and $\delta R_{NL} = \delta V_{NL}/I_{inj}$ are plotted in Fig. 3(d) as a function of V_{3T}. The strong enhancement of the 3 T signals in the excess current regime is clearly observed, as has been reported before in Ref. 15. The contribution of the spin-related signal $\delta R^{\mu}_{3T}/R_{3T}$ to the overall tunnel resistance R_{3T} we plot in the same figure. Whereas $\delta R^{\mu}_{3T}/R_{3T} \approx 0.17$ in the middle of the Esaki feature, it is only ~0.01 for $V_{3T} = 0.28$ V ($I_{inj} = 21\,\mu$A), i.e., for the value for which we observe a strong uniaxial anisotropy in Fig. 2(b). According to Eq. (1), the measured TASP of ~10% would then result in an anisotropic signal in R_{3T} being ~0.2%, i.e., one order of magnitude smaller than the measured value of 2.8%. This allows us to exclude TASP as the origin of a strong uniaxial anisotropy observed in the regime of the excess current.

In summary, we have performed studies of the in-plane TAMR and TASP of (Ga,Mn)As/GaAs spin Esaki tunneling contacts. In the excess current regime, where current flow through localized states in the gap of (Ga,Mn)As prevails, uniaxial symmetry dominates the measured TAMR curves. This is in stark contrast to the direct band-to-band tunneling regime where the cubic anisotropy dominates. This observation is consistent with theoretical calculations showing the importance of impurity states in the (Ga,Mn)As gap for tunneling in (Ga,Mn)As/GaAs Esaki diodes[30] and with calculations showing a similar uniaxial anisotropy in case of tunneling involving a single Mn impurity at the GaAs:Mn/Al(Ga,As)/*p*-type GaAs junction.[29]

This work was partly supported by the German Science Foundation (DFG) via SFB 689, the Japan-Germany

This article is copyrighted as indicated in the article. Reuse of AIP content is subject to the terms at: http://scitation.aip.org/termsconditions. Downloaded to IP: 132.199.100.37 On: Thu, 02 Jul 2015 10:36:54

Strategic International Cooperative Program (Joint Research Type) from JST and DFG (FOR 1483), Grants-in-Aid from JSPS 22226001 and 24684019.

[1]I. Žutić, J. Fabian, and S. Das Sarma, Rev. Mod. Phys. **76**, 323 (2004).
[2]F. J. Jedema, A. T. Filip, and B. J. van Wees, Nature **410**, 345 (2001).
[3]X. Lou, C. Adelmann, M. Furis, S. A. Crooker, C. J. Palmstrøm, and P. A. Crowell, Phys. Rev. Lett. **96**, 176603 (2006).
[4]A. Fert and H. Jaffrès, Phys. Rev. B **64**, 184420 (2001).
[5]J. Fabian, A. Matos-Abiague, C. Ertler, P. Stano, and I. Žutić, Acta Phys. Slovaca **57**, 565 (2007).
[6]M. Tran, H. Jaffrès, C. Deranlot, J.-M. George, A. Fert, A. Miard, and A. Lemaître, Phys. Rev. Lett. **102**, 036601 (2009).
[7]R. Jansen, A. M. Deac, H. Saito, and S. Yuasa, Phys. Rev. B **85**, 134420 (2012).
[8]A. Jain, J.-C. Rojas-Sanchez, M. Cubukcu, J. Peiro, J. C. Le Breton, E. Prestat, C. Vergnaud, L. Louahadj, C. Portemont, C. Ducruet, V. Barski, P. Bayle-Guillemaud, L. Vila, J.-P. Attané, E. Augendre, G. Desfonds, S. Gambarelli, H. Jaffrès, J.-M. George, and M. Jamet, Phys. Rev. Lett. **109**, 106603 (2012).
[9]S. P. Dash, S. Sharma, R. S. Patel, M. P. de Jong, and R. Jansen, Nature **462**, 491 (2009).
[10]R. Jansen, Nat. Mater **11**, 400 (2012).
[11]T. Uemura, K. Kondo, J. Fujisawa, K. Matsuda, and M. Yamamoto, Appl. Phys. Lett. **101**, 132411 (2012).
[12]O. Txoperena, M. Gobbi, A. Bedoya-Pinto, F. Golmar, X. Sun, L. E. Hueso, and F. Casanova, Appl. Phys. Lett. **102**, 192406 (2013).
[13]Y. Song and H. Derry, Phys. Rev. Lett. **113**, 047205 (2014).
[14]H. N. Tinkey, P. Li, and I. Appelbaum, Appl. Phys. Lett. **104**, 232410 (2014).
[15]J. Shiogai, M. Ciorga, M. Utz, D. Shuch, M. Kohda, D. Bougeard, T. Nojima, J. Nitta, and D. Weiss, Phys. Rev. B **89**, 081307(R) (2014).
[16]A. N. Chantis and D. L. Smith, Phys. Rev. B **78**, 235317 (2008).
[17]C. Gould, C. Rüster, T. Jungwirth, E. Girgis, G. M. Schott, R. Giraud, K. Brunner, G. Schmidt, and L. W. Molenkamp, Phys. Rev. Lett. **93**, 117203 (2004).
[18]J. Moser, A. Matos-Abiague, D. Schuh, W. Wegscheider, J. Fabian, and D. Weiss, Phys. Rev. Lett. **99**, 056601 (2007).
[19]J. Wunderlich, T. Jungwirth, B. Kaestner, A. C. Irvine, A. B. Shick, N. Stone, K.-Y. Wang, U. Rana, A. D. Giddings, C. T. Foxon, R. P. Campion, D. A. Williams, and B. L. Gallagher, Phys. Rev. Lett. **97**, 077201 (2006).
[20]M. Tran, J. Peiro, H. Jaffrès, J.-M. George, O. Mauguin, and A. Lemaître, Appl. Phys. Let. **95**, 172101 (2009).
[21]M. Ciorga, M. Schlapps, A. Einwanger, S. Geißler, J. Sadowski, W. Wegscheider, and D. Weiss, New J. Phys. **9**, 351 (2007).
[22]M. Ciorga, A. Einwanger, U. Wurstbauer, D. Schuh, W. Wegscheider, and D. Weiss, Physica E **42**, 2673 (2010).
[23]T. Dietl and H. Ohno, Rev. Mod. Phys. **86**, 187 (2014).
[24]M. Birowska, C. Śliwa, J. A. Majewski, and T. Dietl, Phys. Rev. Lett. **108**, 237203 (2012).
[25]A. Einwanger, M. Ciorga, U. Wurstbauer, D. Schuh, W. Wegscheider, and D. Weiss, Appl. Phys. Lett. **95**, 152101 (2009).
[26]T. Arakawa, J. Shiogai, M. Ciorga, M. Utz, D. Schuh, M. Kohda, J. Nitta, D. Bougeard, D. Weiss, T. Ono, and K. Kobayashi, Phys. Rev. Lett. **114**, 016601 (2015).
[27]A. G. Chynoweth, W. L. Feldmann, and R. A. Logan, Phys. Rev. **121**, 684 (1961).
[28]A. Matos-Abiague, M. Gmitra, and J. Fabian, Phys. Rev. B **80**, 045312 (2009).
[29]M. O. Nestoklon, O. Krebs, H. Jaffres, J.-M. George, J. M. Jancu, and P. Voisin, Appl. Phys. Lett. **100**, 062403 (2012).
[30]P. Pereyra and D. Weiss, Phys. Rev. B **90**, 245310 (2014).
[31]P. Sankowski, P. Kacman, J. A. Majewski, and T. Dietl, Phys. Rev. B **75**, 045306 (2007).
[32]M. Ciorga, M. Utz, D. Schuh, D. Bougeard, and D. Weiss, Phys. Rev. B **88**, 155308 (2013).
[33]J. Shiogai, M. Ciorga, M. Utz, D. Schuh, T. Arakawa, M. Kohda, K. Kobayashi, T. Ono, W. Wegscheider, D. Weiss, and J. Nitta, Appl. Phys. Lett. **101**, 212402 (2012).

This article is copyrighted as indicated in the article. Reuse of AIP content is subject to the terms at: http://scitation.aip.org/termsconditions. Downloaded to IP: 132.199.100.37 On: Thu, 02 Jul 2015 10:36:54